

INFORMATION TO USERS

This was produced from a copy of a document sent to us for microfilming. While the most advanced technological means to photograph and reproduce this document have been used, the quality is heavily dependent upon the quality of the material submitted.

The following explanation of techniques is provided to help you understand markings or notations which may appear on this reproduction.

1. The sign or "target" for pages apparently lacking from the document photographed is "Missing Page(s)". If it was possible to obtain the missing page(s) or section, they are spliced into the film along with adjacent pages. This may have necessitated cutting through an image and duplicating adjacent pages to assure you of complete continuity.
2. When an image on the film is obliterated with a round black mark it is an indication that the film inspector noticed either blurred copy because of movement during exposure, or duplicate copy. Unless we meant to delete copyrighted materials that should not have been filmed, you will find a good image of the page in the adjacent frame.
3. When a map, drawing or chart, etc., is part of the material being photographed the photographer has followed a definite method in "sectioning" the material. It is customary to begin filming at the upper left hand corner of a large sheet and to continue from left to right in equal sections with small overlaps. If necessary, sectioning is continued again—beginning below the first row and continuing on until complete.
4. For any illustrations that cannot be reproduced satisfactorily by xerography, photographic prints can be purchased at additional cost and tipped into your xerographic copy. Requests can be made to our Dissertations Customer Services Department.
5. Some pages in any document may have indistinct print. In all cases we have filmed the best available copy.

University
Microfilms
International

300 N. ZEEB ROAD, ANN ARBOR, MI 48106
.18 BEDFORD ROW, LONDON WC1R 4EJ, ENGLAND

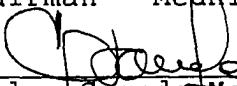
PREVIEW

NUMERICAL ANALYSIS OF THE COMPLETE EIGENVALUE
SOLUTION OF RIDGED WAVEGUIDE.

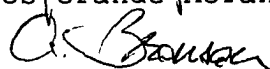
APPROVED:



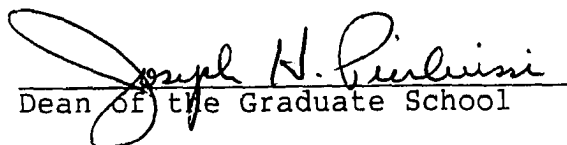
Chairman Mehdi Shadaram



Carlos Grande Moran



Arturo Bronson


Dean of the Graduate School

NUMERICAL ANALYSIS OF THE COMPLETE EIGENVALUE
SOLUTION OF RIDGED WAVEGUIDE.

by

Genaro Granados Tiznado

THESIS

Presented to the faculty of the Graduate School of
The University of Texas at El Paso
in Partial Fullfillment
of the Requirements
for the Degree of

MASTER OF SCIENCE

THE UNIVERSITY OF TEXAS AT EL PASO

Spring/1988

ABSTRACT

In this thesis the complete solution of the ridged waveguide is presented. The derivations of these solutions are the work of James P. Montgomery. His solution was obtained by the formulation of an integral eigenvalue equation which is subsequently solved numerically by application of the Ritz-Garleking method. The significance of the eigenvalue spectrum is discussed and the modes are classified. Equations are given for the electric and magnetic fields. Also the orthogonality property is tested for each case given. Numerical results are also presented.

PREVIEW

TABLE OF CONTENTS

Chapter	Page
1. INTRODUCTION.....	1
2. TE EIGENVALUES SOLUTION.....	3
3. TM EIGENVALUES SOLUTION.....	16
4. ORTHOGONALITY PROPERTY DEMOSTRATION.....	22
5. DISCUSSIONS AND CONCLUSIONS.....	30
REFERENCES.....	39
Appendix.....	
A. TE MODES: ELECTRIC SYMMETRY BOUNDARY.	41
B. TM MODES: ELECTRIC SYMMETRY BOUNDARY.	43
C. FLOW CHART OF THE COMPUTER PRORAM....	45
D. COMPUTER PROGRAM.....	53
CURRICULUN VITAE.....	67

CHAPTER 1

Introduction

Many problems encountered today have demonstrated the necessity of a complete knowledge of a waveguide's eigenvalue spectrum. One such problem is the radiation of waveguide elements in an array environment where higher order modal resonances may create so-called blind spots. Another one is the approach in designing waveguide-to-microstrip transition, where a single-ridged waveguide is a natural transition from waveguide to microstrip. By lowering the height of the waveguide gradually and smoothly, the EM fields are forced to concentrate in a region confined between the ridge and the bottom of the guide.

People who have been involved in this area like Cohn (1) who published in 1947 a paper about the ridged waveguide eigenvalues obtained by using transverse resonance to formulate transcendental equations. The discontinuity susceptance between parallel plate waveguides obtained by Whinney and Jamieson (2) was employed in the calculations. In 1955 Hopfer (3) extended Cohn's work to other aspect ratios by inclusion of a first-order correction factor. Hopfer used a quasi-static solution for the discontinuity susceptance between parallel plates obtained by Marcuvitz (4). In 1966 Pyle (5) extended Hopfer's work by publishing accurate data for any aspect ratio.

Additionally, Pyle included an analysis of error effects. Each of these previous investigations was primarily aimed at the solution for the TE_{n0} eigenvalues. Little was said about the fields of ridged waveguide until 1961 when Getsinger(6) formulated approximate field equations by assuming a TEM mode at the gap and matching only the electric field. Getsinger used the eigenvalues obtained by Hopfer.

In order to perform a complete study of the ridged waveguide this thesis formulates an integral eigenvalue problem. The homogeneous equations are solved numerically by applying the Ritz-Garleking method (7),(8) to yield a generalized matrix eigenvalue problem. The generalized eigenvalue problem is solved by applying a solution obtained by Barlow and Jones (9). The result of this research is the ability to investigate any eigenvalue with its associated field and the approximate error introduced by numerical solution. This ability in turn permits analysis of complex structures requiring such knowledge.

TE Eigenvalues Solution

The geometry of the ridged waveguide is illustrated in Fig. 1. A symmetry plane (S) is assumed about the y coordinate axis. No symmetry has been assumed about the x coordinate axis. Thus, the eigenvalues problem is subdivided into four cases:

- 1) TE to z fields with a magnetic wall at s.
- 2) TE fields with a magnetic wall at the symmetry plane s.
- 3) TM fields with a magnetic wall at the symmetry plane s.
- 4) TM fields with an electric wall at the symmetry plane s.

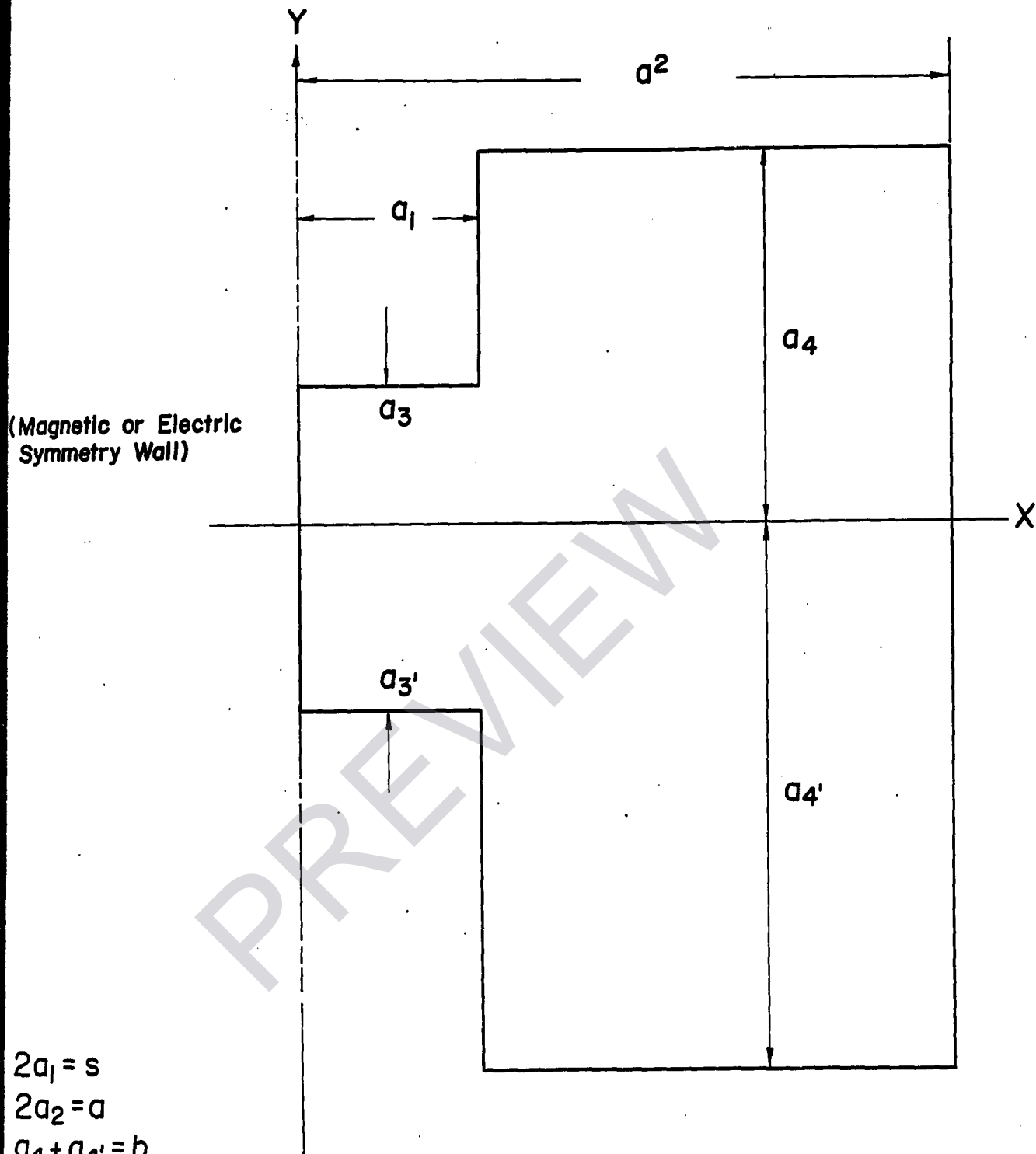
The body of this chapter will be devoted primarily to the fields with a magnetic symmetry plane.

The TE fields are derivable from a hertzian potential of the form:

$$\Pi_n = g(r_T) \cdot \phi(z) \hat{a}_z \quad (2.1)$$

where: $g(r_T)$ = function of the transverse coordinate vector.

$\phi(z)$ = is a function of only the z-coordinate.



$$2a_1 = s$$

$$2a_2 = a$$

$$a_4 + a_4' = b$$

$$a_3 + a_3' = d$$

Fig. 1.

Geometry of Ridged Waveguide

Both scalar function must satisfy the wave equation:

$$\nabla^2 g(r_T) + K_T^2 g(r_T) = 0 \quad (a)$$

$$\phi''(z) + \gamma^2 \phi(z) = 0 \quad (b) \quad (2.2)$$

where: kt = waveguide eigenvalue

γ = propagation constant

$$\gamma = \begin{cases} (K_o^2 - K_T^2)^{1/2}, & K_o > K_T \\ -j(K_T^2 - K_o^2)^{1/2}, & K_T > K_o \end{cases} \quad (2.3)$$

Where the scalar potential functions are related to the electric and magnetic fields by the equations:

$$\vec{E}(r_T) = -j\omega\mu\phi(z)\nabla g(r_T) \times \hat{a}_z \quad (2.4)$$

$$\vec{H}(r_T) = \phi'(z)\nabla g(r_T) + K_T^2 g(r_T)\phi(z)\hat{a}_z \quad (2.5)$$

Often only the transverse components of the field are required, this enable us to simplify the last two equations as:

$$\vec{E}_t(r_T) = \nabla g(r_T) \times \hat{a}_z \quad (2.6)$$

$$\vec{H}_t(r_T) = \gamma \hat{a}_z \times E_t(r_T) \quad (2.7)$$

where: $\gamma = \delta / \mu \omega$

The TE mode boundary conditions are:

$$\hat{a}_n \cdot \nabla g(r_T) = 0 \text{ for metallic boundary.}$$

$$g(r_T) = 0 \text{ for magnetic boundary.}$$

If we apply these equations to the geometry, we are able to divide the potential into two regions.

Region 1 ($0 < x < a_1$):

$$g_r(r_T) = \sum_{n=0}^{\infty} \gamma_{1n} \sin(K_{x1n} X) \cdot \cos\left(\frac{n\pi}{a_3+a_1} (y - a_3)\right) \quad (2.8)$$

$$K_{x1n} = \begin{cases} (K_T^2 - (\frac{n\pi}{a_3+a'_3})^2)^{1/2}, & K_T > \frac{n\pi}{a_3+a'_3} \\ -j((\frac{n\pi}{a_3+a'_3})^2 - K_T^2)^{1/2}, & K_T < \frac{n\pi}{a_3+a'_3} \end{cases} \quad (2.9)$$

Region 2 ($a_1 < x < a_2$):

$$g_2(x_T) = \sum_{n=0}^{\infty} \gamma_{2m} \cos(K_{x2m}(x-a_2)) \cdot \cos(\frac{m\pi}{a_4+a'_4}(y-a_4)) \quad (2.10)$$

$$K_{x2m} = \begin{cases} (K_T^2 - (\frac{m\pi}{a_4+a'_4})^2)^{1/2}, & K_T > \frac{m\pi}{a_4+a'_4} \\ -j((\frac{m\pi}{a_4+a'_4})^2 - K_T^2)^{1/2}, & K_T < \frac{m\pi}{a_4+a'_4} \end{cases} \quad (2.11)$$

Substituting eqs. (2.8) and (2.9) in eqs. (2.6) and (2.7) we can have the electric field for region 1:

$$\vec{E}_1(x_T) = \sum_{n=0}^{\infty} -\gamma_{1n} \left[\left(\frac{n\pi}{a_3+a'_3} \right) \sin(K_{x1n}x) \cdot \sin\left(\frac{n\pi}{a_3+a'_3}(y-a_3)\right) \hat{a}_x + K_{x1n} \cos(K_{x1n}x) \cdot \cos\left(\frac{n\pi}{a_3+a'_3}(y-a_3)\right) \hat{a}_y \right] \quad (2.12)$$

In the same way for region 2:

$$\vec{E}_2(x_T) = \sum_{m=0}^{\infty} -\gamma_{2m} \left[\left(\frac{m\pi}{a_4+a'_4} \right) \cos(K_{x2m}(x-a_2)) \cdot \sin\left(\frac{m\pi}{a_4+a'_4}(y-a_4)\right) \hat{a}_x + K_{x2m} \sin(K_{x2m}(x-a_2)) \cos\left(\frac{m\pi}{a_4+a'_4}(y-a_4)\right) \hat{a}_y \right] \quad (2.13)$$

At this point we need to find the aperture electric field in region 1 and 2 using Fourier series. We can define a Fourier series for a periodic function $f(x)$ that satisfies the Dirichlet conditions and with a fundamental period T as:

$$f(x) = a_0 + \sum_{n=1}^{\infty} \left[a_n \cos \frac{2n\pi x}{T} + b_n \sin \frac{2n\pi x}{T} \right]$$

where:

$$a_0 = \frac{1}{T} \int_{-T/2}^{T/2} f(x) dx$$

$$a_n = \frac{2}{T} \int_{-T/2}^{T/2} f(x) \cdot \cos \frac{2n\pi x}{T} dx$$

$$b_n = \frac{2}{T} \int_{-T/2}^{T/2} f(x) \cdot \sin \frac{2n\pi x}{T} dx$$

Assuming the electric field changes only in the y direction it is possible to define a periodic function $E_{gap}'(y)$. At $x=a_1$ the boundary conditions require that the tangential electric and magnetic fields be continuous. Also, it is required that the tangential electric field vanish on the conducting walls of the ridge. The boundary conditions are applied at a cut off condition ($\gamma = 0$).

Matching the electric field results (eqs. 2.12, 2.13) we get at $x=a_1$ that:

Region 1:

$$\begin{aligned}\vec{E}_1(r_1) = & -\eta_{10} K_{x10} \cos(K_{x10} a_1) \hat{a}_y \\ & - \sum_{n=1}^{\infty} \eta_{1n} K_{x1n} \cos(K_{x1n} a_1) \cdot \cos\left(\frac{n\pi(y-a_3)}{a_3+a'_3}\right) \hat{a}_y \\ & - \sum_{n=1}^{\infty} \eta_{1n} \frac{n\pi}{a_3+a'_3} \sin(K_{x1n} a_1) \cdot \sin\left(\frac{n\pi(y-a_3)}{a_3+a'_3}\right) \hat{a}_x \quad (2.14)\end{aligned}$$

Then the a_0 component can be defined as:

$$a_0 = \eta_{10} K_{x10} \cos(K_{x10} a_1) = \frac{1}{a_3+a'_3} \int_{-a'_3}^{a_3} E_{GAP}(y') dy'$$

Also the a_n component is:

$$\begin{aligned}a_n = & -\eta_{1n} K_{x1n} \cos(K_{x1n} a_1) = \frac{2}{a_3+a'_3} \int_{-a'_3}^{a_3} E_{GAP}(y') \cos\left(\frac{2n\pi(y'-a_3)}{a_3+a'_3}\right) dy' \\ & - \eta_{1n} K_{x1n} \cos(K_{x1n} a_1) \cdot \left(\frac{a_3+a'_3}{2}\right) = \int_{-a'_3}^{a_3} E_{GAP}(y') \cos\left(\frac{2n\pi(y'-a_3)}{a_3+a'_3}\right) dy' \quad (2.15)\end{aligned}$$

For region 2:

$$\begin{aligned}\vec{E}_2(r_2) = & \eta_{20} K_{x20} \sin(K_{x20} (a_1 - a_2)) \hat{a}_y \\ & + \sum_{m=1}^{\infty} \eta_{2m} K_{x2m} \sin(K_{x2m} (a_1 - a_2)) \cdot \cos\left(\frac{m\pi(y-a_4)}{a_4+a'_4}\right) \hat{a}_y \\ & + \sum_{m=1}^{\infty} -\eta_{2m} K_{x2m} \cos(K_{x2m} (a_1 - a_2)) \cdot \sin\left(\frac{m\pi(y-a_4)}{a_4+a'_4}\right) \hat{a}_x \quad (2.16)\end{aligned}$$